Final Report
#01-F-1987

NEW DISCHARGE PUMPING METHOD FOR CO_2 LASER

FINAL TECHNICAL REPORT

Sponsored by

Defense Advanced Research Projects Agency (DoD)

Defense Small Business Innovation Research Program

ARPA Order No. 5916

Issued by U.S. Army Missile Command Under
Contract #DAAH01-86-C-1074

Contract Dates: September 26, 1986 - May 30, 1987

Prepared by

Dr. Jonah H. Jacob

617-547-1122

Science Research Laboratory, Inc.

15 Ward Street Somerville MA 02143

(2)

NEW DISCHARGE PUMPING METHOD FOR CO_2 LASERS

FINAL TECHNICAL REPORT

Sponsored by

Defense Advanced Research Projects Agency (DoD)

Defense Small Business Innovation Research Program

ARPA Order No. 5916

Issued by U.S. Army Missile Command Under
Contract #DAAH01-86-C-1074

Contract Dates: September 26, 1986 - May 30, 1987

Prepared by

Dr. Jonah H. Jacob

Science Research Laboratory, Inc.
15 Ward Street
Somerville, MA 02143

617-547-1122

"The views and conclusions contained in this document are those of the authors and should not be interpreted as representing the official policies, either expressed or implied, of the Defense Advanced Research Projects Agency or the U.S. Government."

UNCLASSIFIED
SECURITY CLASSIFICATION OF THIS PAGE

REPORT DOCUMENTATION PAGE

1a REPORT SECURITY CLASSIFICATION: Unclassified	1b RESTRICTIVE MARKINGS: None AD-A181 635
2a SECURITY CLASSIFICATION AUTHORITY: N/A	3 DISTRIBUTION / AVAILABILITY OF REPORT: Unlimited
2b DECLASSIFICATION / DOWNGRADING SCHEDULE: N/A	
4. PERFORMING ORGANIZATION REPORT NUMBER(S): 01/F/1987	5 MONITORING ORGANIZATION REPORT NUMBER(S)
6a. NAME OF PERFORMING ORGANIZATION: Science Research Laboratory; 6b. OFFICE SYMBOL (If applicable)	7a. NAME OF MONITORING ORGANIZATION: U.S. Army Missile Command
6c. ADDRESS (City, State, and ZIP Code): 15 Ward St. Somerville, MA 02143	7b. ADDRESS (City, State, and ZIP Code): AMSMI-PC-BFA/DARPA Proj OFC Ms. Goldie Hill Redstone Arsenal, AL 35898-5280
8a. NAME OF FUNDING / SPONSORING ORGANIZATION: DARPA; 8b. OFFICE SYMBOL (If applicable)	9 PROCUREMENT INSTRUMENT IDENTIFICATION NUMBER: DAAH01-86-C-1074
8c. ADDRESS (City, State, and ZIP Code): 1400 Wilson Blvd. Arlington, VA 22209	10 SOURCE OF FUNDING NUMBERS: PROGRAM ELEMENT NO; PROJECT NO: PAN:RADB1; TASK NO: 6; WORK UNIT ACCESSION NO

11 TITLE (Include Security Classification)

New Discharge Pumping Method for CO_2 Lasers (U)

12. PERSONAL AUTHOR(S): Jonah Jacob

13a TYPE OF REPORT	13b. TIME COVERED	14. DATE OF REPORT (Year, Month, Day)	15 PAGE COUNT
Final Technical	FROM 9/26/86 TO 5/30/87	May 27, 1987	49

16 SUPPLEMENTARY NOTATION

17 COSATI CODES			18 SUBJECT TERMS (Continue on reverse if necessary and identify by block number)
FIELD	GROUP	SUB-GROUP	

19 ABSTRACT (Continue on reverse if necessary and identify by block number)

A new pulsed laser discharge concept is proposed to meet military and civilian requirements for efficient operation of compact, high energy CO_2 lasers. This discharge concept promises pulse lengths of up to 100 microseconds duration scalability to multi-kilojoule single pulsed energy, high volumetric efficiency ($\geq$ 50 Joules/liter-atm) and high electrical efficiency ($\geq$ 20%). This discharge concept relies on a new method for maintaining discharge stability for long pulse durations. This new CO_2 laser discharge concept promises increased efficiency, repetition rate, laser pulse length, extracted energy per unit volume and reliability. The concept utilizes a current source to insure volumetric stability. Such a source will not stabilize the discharge against streamer formation. Streamer formation can be inductively inhibited by the use of RF. Hence an RF current source could result in a more stable laser discharge.

20. DISTRIBUTION / AVAILABILITY OF ABSTRACT	21 ABSTRACT SECURITY CLASSIFICATION
☒ UNCLASSIFIED/UNLIMITED ☐ SAME AS RPT ☐ DTIC USERS	Unclassified
22a. NAME OF RESPONSIBLE INDIVIDUAL: Jonah Jacob	22b. TELEPHONE (Include Area Code): 617-547-1122; 22c. OFFICE SYMBOL

DD FORM 1473, 84 MAR — 83 APR edition may be used until exhausted. All other editions are obsolete.

SECURITY CLASSIFICATION OF TH

TABLE OF CONTENTS

NEW DISCHARGE PUMPING METHOD FOR CO_2 LASERS

ABSTRACT

A new pulsed laser discharge concept is proposed to meet military and civilian requirements for efficient operation of compact, high energy CO_2 lasers. This discharge concept promises pulse lengths of up to 100 microseconds duration, scalability to multi-kilojoule single pulsed energy, high volumetric efficiency (≥ 50 Joules/liter-atm) and high electrical efficiency (≥ 20%). This discharge concept relies on a new method for maintaining discharge stability for long pulse durations. This new CO_2 laser discharge concept promises increased efficiency, repetition rate, laser pulse length, extracted energy per unit volume and reliability. The concept utilizes a current source to insure volumetric stability. Such a source will not stabilize the discharge against streamer formation. Streamer formation can be inductively inhibited by the use of RF. Hence an RF current source could result in a more stable laser discharge.

1.0 INTRODUCTION

A new laser discharge concept has been identified which is compatible with military and civilian applications which require efficient operation of compact high power CO_2 lasers. This concept is based on a new discharge method which will insure the macroscopic and microscopic stability of the discharge at high pump power density and for long pulse lengths. This discharge concept promises pulse lengths of up to 100 microseconds duration, scalability to multi-kilojoule single pulse energy, high volumetric efficiency (up to 50 Joules/liter-atm), and high electrical efficiency. This new discharge method utilizes spatially uniform x-ray or UV preionization of the laser medium followed by a discharge pulse which initially supplies a voltage across the discharge electrodes, approximately equal to twice the sustaining voltage, to avalanche the electron density uniformly to 10^{12} electrons/cm^3. The current source drive prevents volumetric discharge instabilities. The oscillating discharge voltage prevents localized electron density avalanche by controlling the ionization and recombination during the peaks and valleys of waveform and by limiting, by inductance, the localization of discharge current.

In Section 2 of this report the analytical and numerical model of this new CO_2 laser discharge concept is presented, regions of stable discharge operation and efficient CO_2 laser performance will be identified. In Section 3 this model is applied to the special case of a CO_2 laser discharge. Section 4 discusses inductive stabilization by the use of RF. Section 5 discusses the impact of RF on the CO_2 laser

operation. In Section 6 this report a conceptual design for a single pulse CO_2 laser experiment which can be used to validate this new discharge concept is presented.

2.0 VOLUMETRIC DISCHARGE STABILITY MODEL

Two rate equations are important in determining the stability of the discharge. The first is the electron production and loss

$$\frac{dn_e}{dt} = \nu n_m n_e - \alpha n_e^2 - \beta n_e \qquad (1)$$

and the second is the metastable production and loss

$$\frac{dn_m}{dt} = \langle \sigma v \rangle n_e n_a - n_m/\tau_m \qquad (2)$$

where n_e is the electron density, n_m is the metastable density, α is the recombination rate, β is the attachment rate, $\langle \sigma v \rangle$ is the electron impact metastable production rate constant and τ_m is the metastable lifetime. The ionization rate constant ν in Eq. (1) is assumed to be the result of metastable ionization. Since the metastable levels have a much smaller ionization energy than the ground state the ionization rate of the discharge is dominated by electron impact ionization of the metastables. The stability of Eqs. (1) and (2) will be analyzed for both current and voltage sources and for a voltage source having an arbitrary impedence.

2.1 STABILITY OF THE DISCHARGE DRIVEN BY A VOLTAGE SOURCE

The rate Eqs. (1) and (2) are a pair of nonlinear simultaneous differential equations. If the discharge electric field (voltage source) is constant in time they can be solved by a perturbation analysis around the steady state, i.e.,

$$n_e = n_{e0} + \delta n_e \qquad (3)$$

and

$$n_m = n_{m0} + \delta n_m \tag{4}$$

Substituting Eqs. (3) and (4) into (1) and (2) and seeking solutions of the form $\delta n_{em} \sim \exp(-i\omega t)$ results in the following quadratic equation in ω

$$\omega^2 + i\omega\left(\alpha n_{e0} + \frac{1}{\tau_m}\right) + \frac{\beta}{\tau_m} = 0 \tag{5}$$

The two roots of (5) are

$$\omega_{\pm} = -\frac{i}{2}\left[\left(\alpha n_{e0} + \frac{1}{\tau_m}\right) \pm \left\{\left(\alpha n_{e0} + \frac{1}{\tau_m}\right)^2 + \frac{4\beta}{\tau_m}\right\}^{1/2}\right] \tag{6}$$

From Eq. (6) one can draw the following conclusions for a voltage source driven discharge

(a) The discharge is marginally stable when the attachment rate β is zero. The two roots are $\omega_1 = 0$ (marginally stable) and $\omega_2 = -i(\alpha n_{e0} + 1/\tau_m)$ decaying.

(b) For a finite attachment rate there are no stable roots. For a recombination dominated discharge, the decaying root is the same as for the case with zero attachment and growing root is given by

$$\omega_1 = \beta\,(1 + \alpha n_{e0}\,\tau)^{-1}$$

To verify these solutions Eqs. (1) and (2) have been numerically integrated and the results are shown in Figs. 1, 2 and 3.

Figure 1 shows plots of n_e and n_m as a function of time for the special case of zero attachment. n_{e0} was initialized to 10^{14} cm^{-3} and n_{m0} to zero. The electron density decreases rapidly initially until

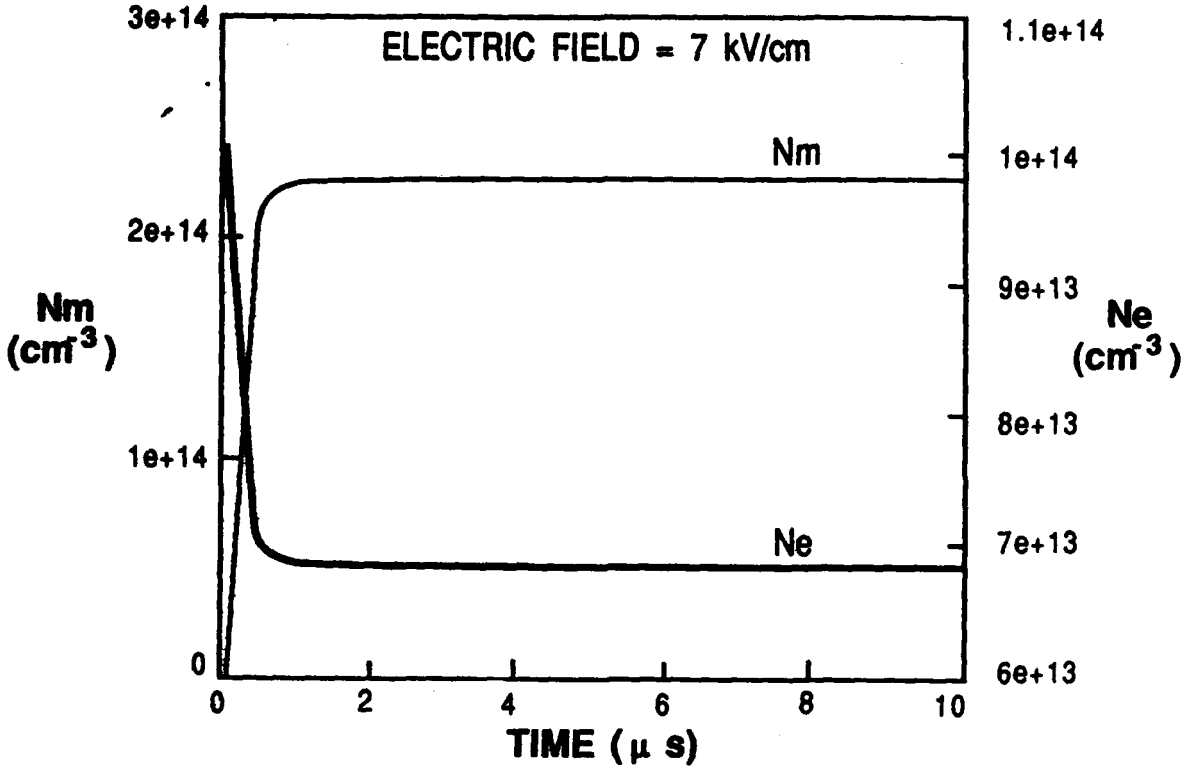
ELECTRIC FIELD = 7 kV/cm
Nm
Ne
3e+14
2e+14
1e+14
0
Nm (cm-3)
1.1e+14
1e+14
9e+13
8e+13
7e+13
6e+13
Ne (cm-3)
0
2
4
6
8
10
TIME (μ s)

Figure 1

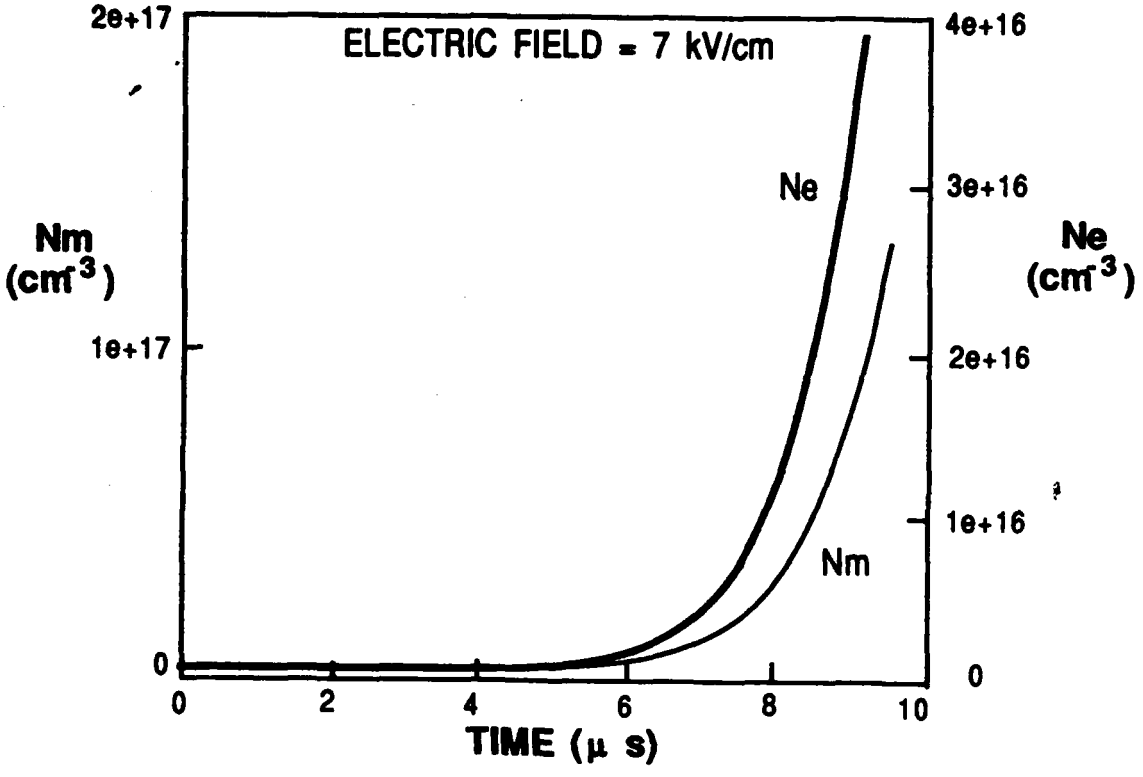
ELECTRIC FIELD = 7 kV/cm
Ne
Nm
Nm
(cm-3)
Ne
(cm-3)
2e+17
1e+17
0
4e+16
3e+16
2e+16
1e+16
0
0
2
4
6
8
10
TIME (μ s)

Figure 2

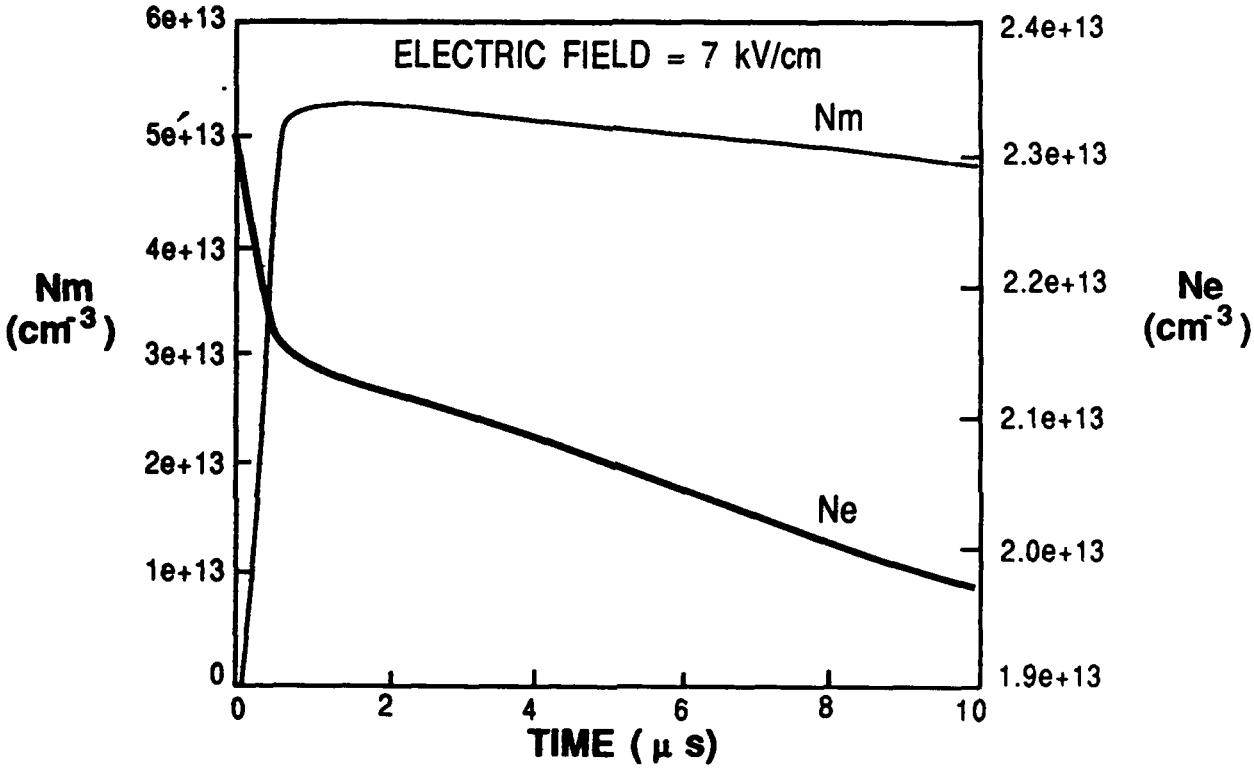
ELECTRIC FIELD = 7 kV/cm
Nm
Ne
Nm (cm-3)
Ne (cm-3)
6e+13
5e+13
4e+13
3e+13
2e+13
1e+13
0
2.4e+13
2.3e+13
2.2e+13
2.1e+13
2.0e+13
1.9e+13
0
2
4
6
8
10
TIME (μ s)

Figure 3

the metastable density reaches a steady state value of about 2.2 x 10^{14}. The electron density then stabilizes at a density of 7 x 10^{13} cm^{-3}.

Figure 2 shows the result of introducing a small amount of attachment (i.e., $\beta = 10^5$ sec^{-1}). Again the initial n_{e0} and n_m were 10^{14} cm^{-3} and zero notice that the discharge is unstable. However, if the initial electron density is chosen to be 2 x 10^{13} cm^{-3} the discharge decays. By inspecting Eqs. (1) and (2) in the presence of attachment it can be shown that there exists critical electron density

$$n_{ec} = \beta \, (\nu \, \langle \sigma v \rangle \, \tau_m n_a - \alpha)^{-1}$$

For an initial electron density, $n_{e1} > n_{ec}$ the discharge is unstable and for $n_{e1} < n_{ec}$ the discharge is quenched.

2.2 STABILITY OF A DISCHARGE DRIVEN BY A CURRENT SOURCE

Next, Eqs. (1) and (2) will be investigated for the case of constant current source. A constant current source implies that

$$J_D = n_e \, v_d e = \text{const}$$

and any perturbation in the electron density must immediately result in a perturbation of the drift velocity v_d, i.e.,

$$\delta(v_d) = - v_{d0} \, \frac{\delta n_e}{n_{e0}} \qquad (7)$$

This change in v_d can only result from change in the electric

field E

$$\delta E = (\delta v_d)\left(\frac{\partial v_{do}}{\partial E}\right)^{-1} = -\frac{v_{do}}{v_{do}}\frac{\delta n_{eo}}{n_{eo}} \tag{8}$$

For CO_2 laser mixtures $(\partial v_{do}/\partial E) > 0$ and so Eq. (8) implies that an increase in n_e leads to a decrease in the electric field which leads to subsequent decrease in production of the metastables and electrons.

The linearized rate equations for a current source drive can be written as

$$\frac{d(\delta n_m)}{dt} = n_{eo}(n_{mo}\nu' - n_{eo}\alpha')\ \delta E + \nu n_{eo}\ (\delta n_m) + (\nu n_{mo} - 2\alpha n_{eo})\delta n_e \tag{9}$$

$$\frac{d(\delta n_m)}{dt} = \langle\sigma v\rangle\ n_a n_{eo}(\delta E) - \frac{1}{\tau_m}\ (\delta n_m) + \langle\sigma v\rangle\ n_a(\delta n_e) \tag{10}$$

Substituting Eq. (8) into (9) and (10) and assuming the form $\delta n_{em} \sim \exp(-i\omega t)$ and that α is small one gets

$$\nu n_{eo}(\delta n_m) + \left(i\omega + \nu n_{mo} - 2\alpha n_{eo} - \frac{v_{do} n_{mo}\nu'}{v_d'} + \frac{\alpha' n_{eo}\ v_{do}}{v_d}\right)\delta n_e = 0 \tag{11}$$

and

$$i\omega - \frac{1}{\tau}\ (\delta n_m) + \left(\langle\sigma v\rangle n_a - \frac{n_a v_{do}\langle\sigma v\rangle'}{v_d}\right)\delta n_e = 0 \tag{12}$$

Equations (11) and (12) can be combined to give

$$\omega^2 + i\omega\left(\alpha n_{eo} + \frac{1}{\tau_m} + \frac{v_{do}\ n_{mo}\ \nu'}{v_d} - \alpha\ \frac{v_{do} n_{eo}}{v_d'}\right) - \frac{\nu\ v_{do}\ n_{mo}}{v_d\ \tau_m}\left(\frac{\nu'}{\nu} + \frac{\langle\sigma v\rangle'}{\langle\sigma v\rangle} - \frac{\alpha'}{\alpha}\right) \tag{13}$$

The two roots of the equations are

$$\omega_{\pm} = -\frac{i}{2}\left[A \pm (A^2 + 4B)^{1/2}\right] \tag{14}$$

where $$A = \alpha n_{e_0} + \frac{1}{\tau_m} + \frac{v_{d_0}\, n_{m_0}\, \nu'}{v_d} - \alpha' \frac{v_{d_0}}{v_d'}\, n_{e_0} \tag{15}$$

and $$B = -\frac{\nu\, v_{d_0}\, n_{m_0}}{v_d'\, \tau_m}\left(\frac{\nu'}{\nu} + \frac{\langle\sigma v\rangle}{\langle\sigma v\rangle} - \frac{\alpha'}{\alpha}\right) \tag{16}$$

At the electric fields that result in efficient laser operation both ν' and $\langle\sigma v\rangle$ are positive and α' is negative, and hence B is negative and both roots of Eq. (14) results decaying exponentials, i.e. the system becomes absolutely stable. Physically this comes about because any increase in the current will result in a decrease in the electric field and hence in the rate constants for the metastable production and ionization will decrease. In the presence of attachment Eq. (13) becomes

$$\omega^2 + i\omega A + \left(\frac{\beta}{\tau_m} + B\right) = 0 \tag{17}$$

So when $\beta > |B\tau_m|$ the one of the roots are unstable, when $\beta = |B\tau_m|$ the discharge is marginally stable and when $\beta < |B\tau_m|$ the discharge is absolutely stable. Physically Eq. (17) says that the discharge is marginally stable if the electron production rate is not a function of the electric field. However, if the electron production rate decreases as the electric field increases (i.e., $\beta < |\tau_m B|$) the discharge is stable and if the electron production rate increases as the electric field decreases the discharge is unstable

2.3 FINITE IMPEDENCE VOLTAGE SOURCE

In practice one does not have either a voltage or a current source and so it is important to consider the effect of a finite impedence circuit on the stability of the laser discharge. A simplified circuit of the discharge and power supply is shown in Fig. 4. The power supply is assumed to be a voltage source V with an internal impedence ρ. The current J through the discharge is given by

$$J = (V - E)/\rho \tag{18}$$

where E is the electric field in the discharge. For simplicity the discharge is assumed to be a cubic centimeter. The perturbed current δJ can be written as

$$\delta J = - \delta E/\rho = e\, v_{d0}\, \delta n_e + e\, n_e\, \delta v_{d0}$$

or

$$\delta E_0 = - e v_{d0} (\delta n_e) \left(\frac{1}{\rho} + e\, n_e\, v_{d0} \right)^{-1} \tag{19}$$

Comparing this to Eq. (8) one finds that the stability criteria developed in the previous section are valid provided v_d is replaced by

$$v_{d1} \rightarrow v_d + \frac{v_{d0}}{e \rho n_{e0}}$$

GENERAL CIRCUIT MODEL

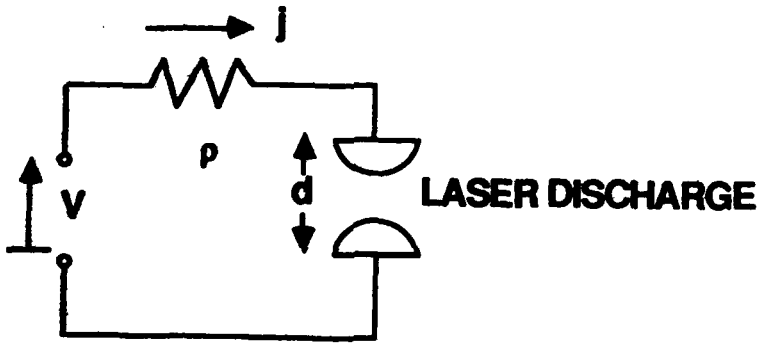

Figure 4

or
$$v_{d1}' \rightarrow v_d' + \frac{v_{do}}{E} \frac{\rho_{disc}}{\rho} \tag{20}$$

where
$$\rho_{disc} = \frac{E}{J} \tag{21}$$

It is interesting to note that for a PFN supply $\rho_{disc} = \rho$ and equation predicts that B as defined (16) decreases approximately by a factor of two. Also as $\rho \rightarrow 0$, $v_{d1} \rightarrow \infty$ and the stability criteria for a voltage source are recovered. When $\rho \rightarrow \infty$, $v_{d1} \rightarrow v_d$ and the stability criteria for a current source are recovered.

The volumetric discharge stability analysis presented in this section is summarized in Table I for the three discharge sources, voltage current and resistive sources. The voltage source is marginally stable for a discharge whose electron loss is only via recombination, any attachment, however, small results in an unstable discharge. The current and resistive sources have stable operating regions. The stable region decreases as the attachment rate increases and as the resistance of the source decreases. In the remainder of this section these regions of stable operation will be evaluated for the special case of a CO_2 laser discharge.

TABLE I

VOLUMETRIC DISCHARGE STABILITY

CONCLUSIONS

	ELECTRON LOSS MECHANISM		
DISCHARGE POWER SOURCE	RECOMBINATION (ZERO ATTACHMENT)	ATTACHMENT DOMINATED	RECOMBINATION AND ATTACHMENT
• VOLTAGE SOURCE	— MARGINALLY STABLE	— UNSTABLE	— UNSTABLE
• CURRENT SOURCE	— STABLE OPERATING REGION*	— STABLE OPERATING REGION*	— STABLE OPERATING REGION*
• RESISTIVE SOURCE	— STABLE OPERATION REGION**	— STABLE OPERATING REGION**	— STABLE OPERATING REGION**

* $|B| > \beta / \tau_m$ where $B = -\nu \frac{n_{mo}}{\tau_m} \frac{V_d}{V_{d'}} \left(\frac{\langle \sigma v \rangle'}{\langle \sigma v \rangle} + \frac{\nu'}{\nu} - \frac{\alpha'}{\alpha} \right)$

** $\frac{V_{d'}}{V_d} \longrightarrow \frac{V_{d'}}{V_d} + \frac{1}{E} \left(\frac{\rho_{disc}}{\rho} \right)$

3.0 MODELLING THE CO_2 LASER DISCHARGE

The discharge model developed so far will be applied to the specific case of a CO_2 laser discharge. Before this can be done, however, one has to know the relevant rate constants for the CO_2 mixture as a function of electric field. The mixture of choice for this effort is a 3/2/1, $He/N_2/CO_2$ mixture. The rate constants for the ionization and excitation of the electronic states of N_2, the fraction of discharge energy that goes into vibration excitation, the drift velocity and electron temperature as predicted by the Boltzmann code are shown in Figs. 5 and 6 . From Fig. 5 which is a plot of T_e, v_d and efficiency of exciting the vibrational levels of N_2, it is clear that efficient CO_2 operation occurs between 5-10 kV/cm.

Figure 6 shows the variation ν and $\langle \sigma v \rangle$ as a function of the electric field. Also shown in Fig. 6 is the curve for the ionization from the ground state. The curve for $\langle \sigma v \rangle$ shown in Fig. 6 is the total excitation rate constant for all the electronic levels. This was chosen since it is difficult to identify the relevant metastable or electronic state that will be subsequently ionized. It is probable that this state will be a high lying state such as the C state of N_2. The metastable ionization rate constant ν has the same shape as the electron impact ionization of the N_2 (a Σ_u),[1] its magnitude, however, was increased by 10^2. Since this state is about 9 eV below the ionization level of N_2 as opposed to the C level which is only 6 eV below the ionization level. From this figure it is clear that $\nu_a \ll \nu$ and so for any reasonable metastable density ($n_m > 10^{12}$ cm^{-3}) the metastable ionization will be dominant. Figure 7 shows the

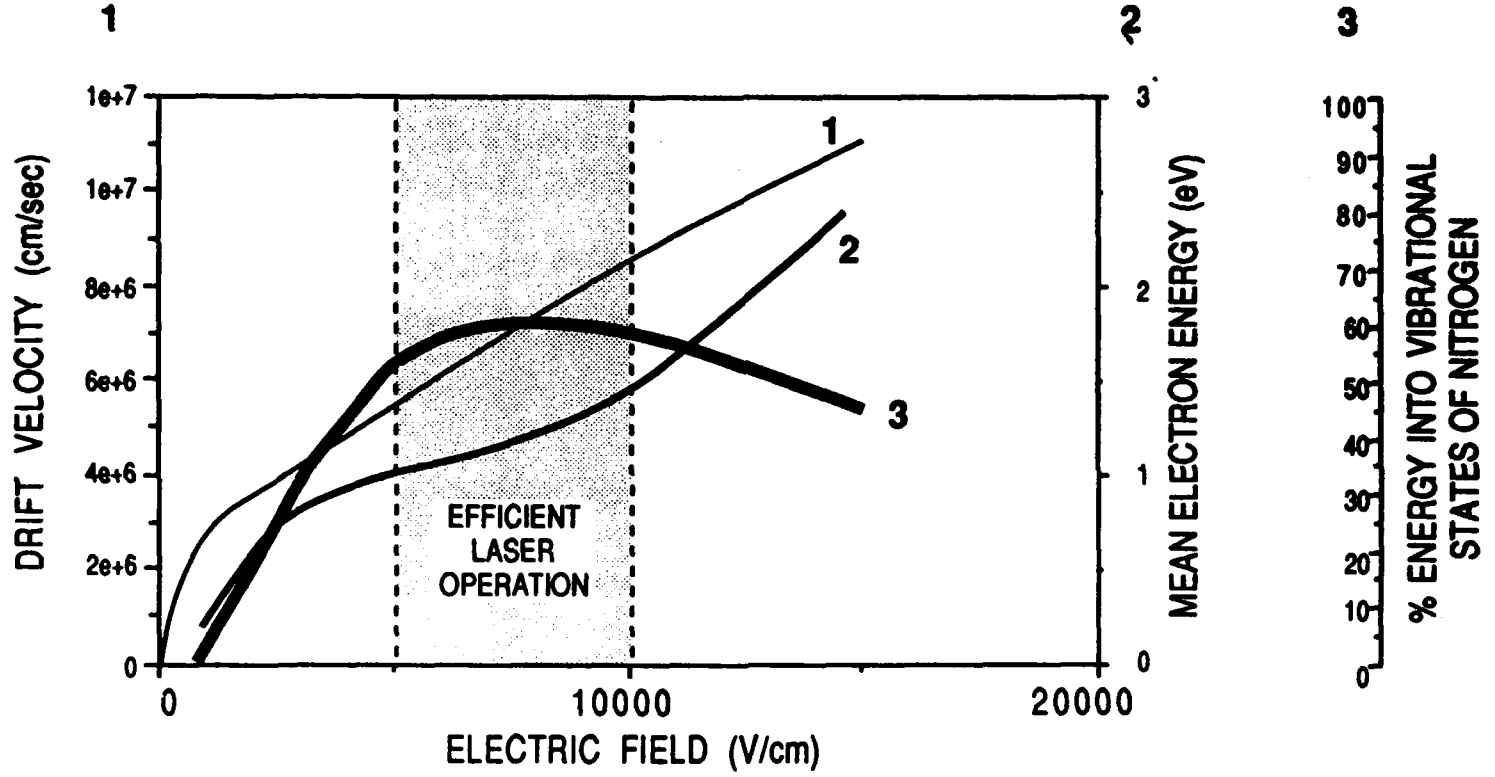
1
2
3
1e+7
1e+7
8e+6
6e+6
4e+6
2e+6
0
DRIFT VELOCITY (cm/sec)
3
2
1
0
MEAN ELECTRON ENERGY (eV)
100
90
80
70
60
50
40
30
20
10
0
% ENERGY INTO VIBRATIONAL STATES OF NITROGEN
1
2
3
EFFICIENT LASER OPERATION
0
10000
20000
ELECTRIC FIELD (V/cm)

Figure 5

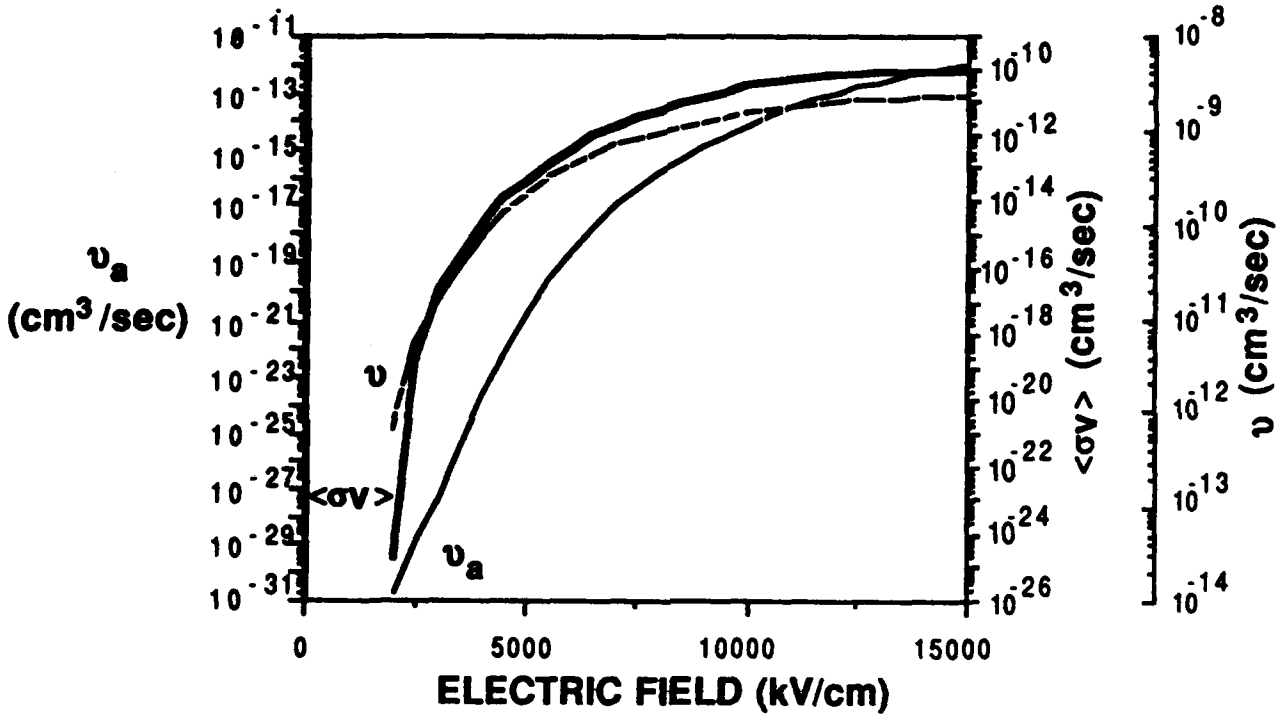
υ_a (cm^3/sec)
10^{-11}
10^{-13}
10^{-15}
10^{-17}
10^{-19}
10^{-21}
10^{-23}
10^{-25}
10^{-27}
10^{-29}
10^{-31}
10^{-10}
10^{-12}
10^{-14}
10^{-16}
10^{-18}
10^{-20}
10^{-22}
10^{-24}
10^{-26}
10^{-8}
10^{-9}
10^{-10}
10^{-11}
10^{-12}
10^{-13}
10^{-14}
<σv> (cm^3/sec)
υ (cm^3/sec)
υ
<σv>
υ_a
0
5000
10000
15000
ELECTRIC FIELD (kV/cm)

Figure 6

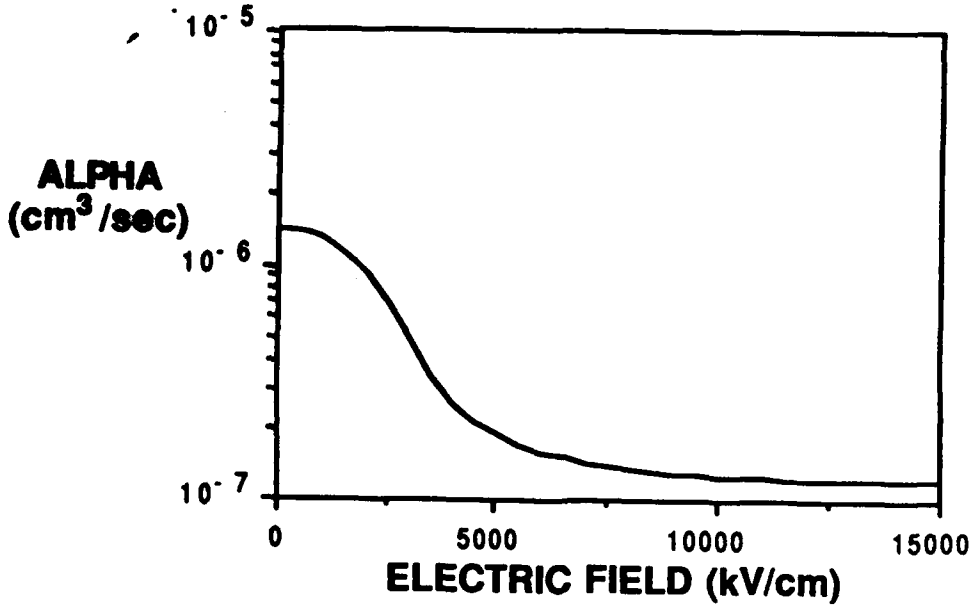
10- 5
ALPHA
(cm3 /sec)
10- 6
10- 7
0
5000
10000
15000
ELECTRIC FIELD (kV/cm)

Figure 7

recombination coefficient as a function of the electric field. Measurements of the recombination coefficient for a 3/2/1 laser has been made for electric field strengths between 2.5 and 5 kV/cm.[1] The curve shown in Fig. 7 make use of these measurements.

3.1 REGIONS OF STABLE OPERATION FOR A CO_2 LASER DISCHARGE

Combining the rate constants predicted by the Boltzmann code with the stability analysis one can identify regions of stable discharge operation for the special case of a CO_2 laser. Figure 8 is a plot where $C = (\beta/\tau_m + B)$, as a function of electric field for an electron density of 10^{12} cm^{-3} and zero attachment. As discussed earlier the discharge is marginally stable when $C = 0$ unstable when $C > 0$ and absolutely stable when $C < 0$. The stable and unstable regions have been identified in Fig. 8. For zero attachment the discharge is marginally stable or absolutely stable as predicted by the stability analysis. For a voltage source with zero internal resistance the discharge is marginally stable. When the pulsed power impedence is equal to the discharge impedence the discharge is absolutely stable between 5-15 kV/cm and marginally stable for electric fields below 5 kV/cm. For electric fields > 15 kV/cm the discharge will probably become unstable because $C > 0$. This is because ν becomes negative. The discharge stability at these high electric fields have not been investigated because it is of little interest for the CO_2 lasers.

In Fig. 9 one sees the effect of adding some attachment. One immediately sees that the case of $\rho = 0$ (voltage source) which was marginally stable before is now unstable however the case where $\rho = \rho_{disc}$ and $\rho = \infty$ (current source) still have stable operating regions

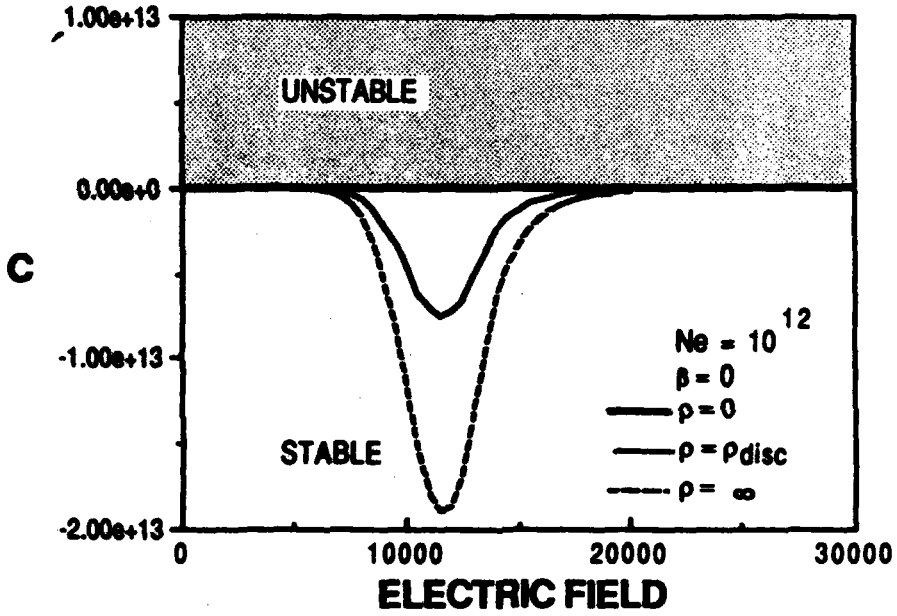
1.00e+13
UNSTABLE
0.00e+0
C
-1.00e+13
STABLE
-2.00e+13
0
10000
20000
30000
ELECTRIC FIELD
Ne = 10 12
β = 0
ρ = 0
ρ = ρdisc
ρ = ∞

Figure 8

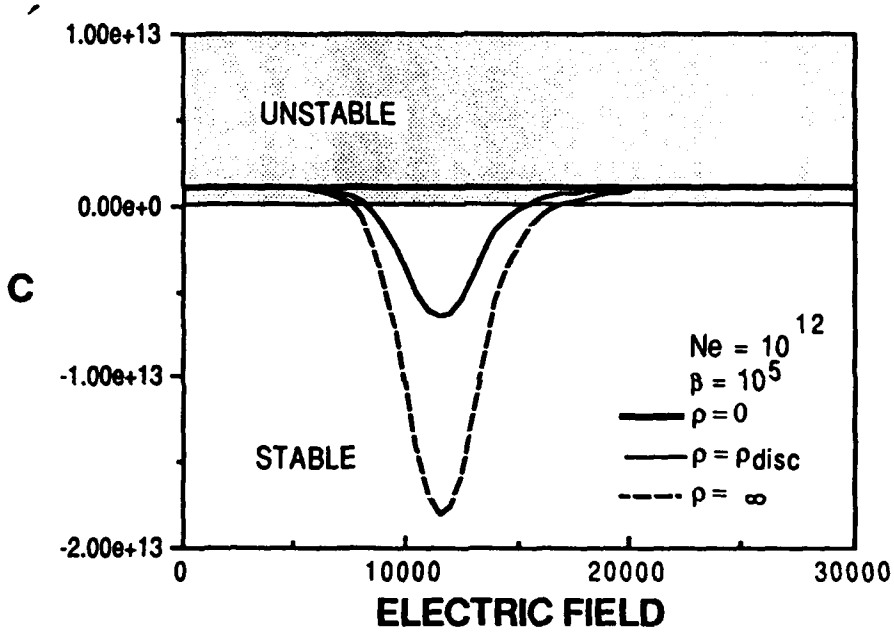
1.00e+13
0.00e+0
-1.00e+13
-2.00e+13
C
UNSTABLE
STABLE
Ne = 10 12
β = 10 5
ρ = 0
ρ = ρdisc
ρ = ∞
0
10000
20000
30000
ELECTRIC FIELD

Figure 9

between 7 and 13 kV/cm. By inspecting Eq. (16) it is clear that the discharge becomes more stable as n_e increases. This is graphically shown in Fig. 10. In fact for $n_e < 10^{11}$ cm^{-3} and $\beta = 2 \times 10^5$ sec^{-1} the discharge is unstable for all values of electric field, this can be seen in Fig. 11. So for small values of n_e and electric fields > 15 kV/cm the secondary electron density will rapidly increase until n_e is large enough and the discharge becomes stable. During this rapid growth of n_e streamers can form, and the discharge can go unstable. To prevent this from happening the initial spatial distribution of n_e must be uniform, further by having an RF source such streamer formation can be inhibited.

The rate Eq. (1) and (2) has been solved simultaneously with the circuit Eq. (18) for the special case of a 3/2/1, $He/CO_2/N_2$ laser discharge. This code also makes use of the rate constants and secondary electron parameters shown in Figs. 5, 6 and 7. The predictions of this code are plotted in Figs. 12 and 13. Figure 12 shows the temporal variation of n_e and E for the circuit impedence of 10^4 Ω. Such an impedence is somewhat larger than the discharge impedence of 8×10^3 Ω. The initial electron density was assumed to be 10^{12} cm^{-3}. The electron density increases by about 10% to 1.08×10^{12} cm^{-3} and the electric field decreases from its initial value of 9 kV/cm to slightly less than 8.5 kV/cm. The temporal variation of C is also shown in Figs. 12 and 13. For the case shown in Fig. 12 C is negative and such a discharge is stable. This discharge clearly becomes unstable when ρ is reduced to 1 Ω. For this case the initial value of C is positive indicative of an unstable discharge. The electron

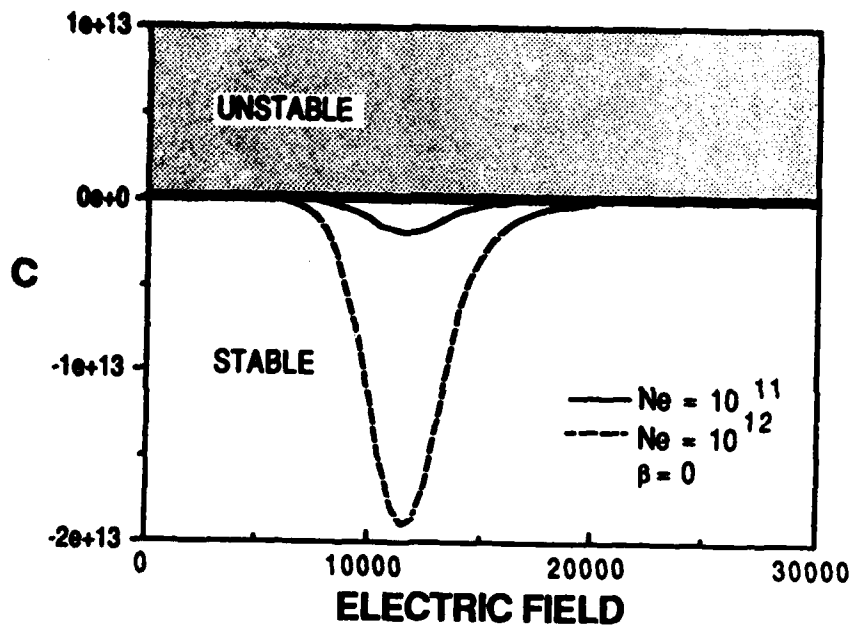
1e+13
UNSTABLE
0e+0
C
-1e+13
STABLE
-2e+13
Ne = 10 11
Ne = 10 12
β = 0
0
10000
20000
30000
ELECTRIC FIELD

Figure 10

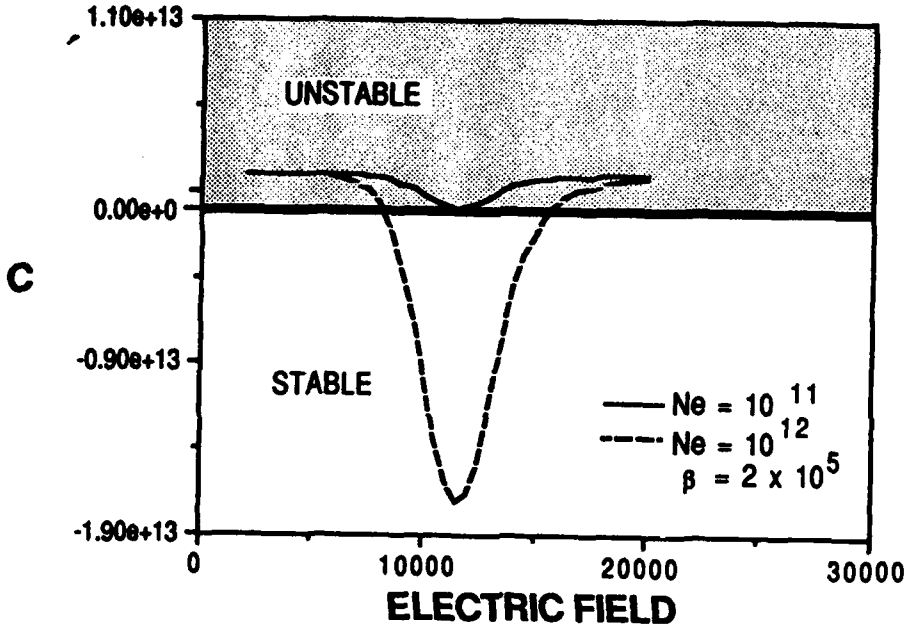
1.10e+13
UNSTABLE
0.00e+0
C
-0.90e+13
STABLE
Ne = 10 11
Ne = 10 12
β = 2 x 10 5
-1.90e+13
0
10000
20000
30000
ELECTRIC FIELD

Figure 11

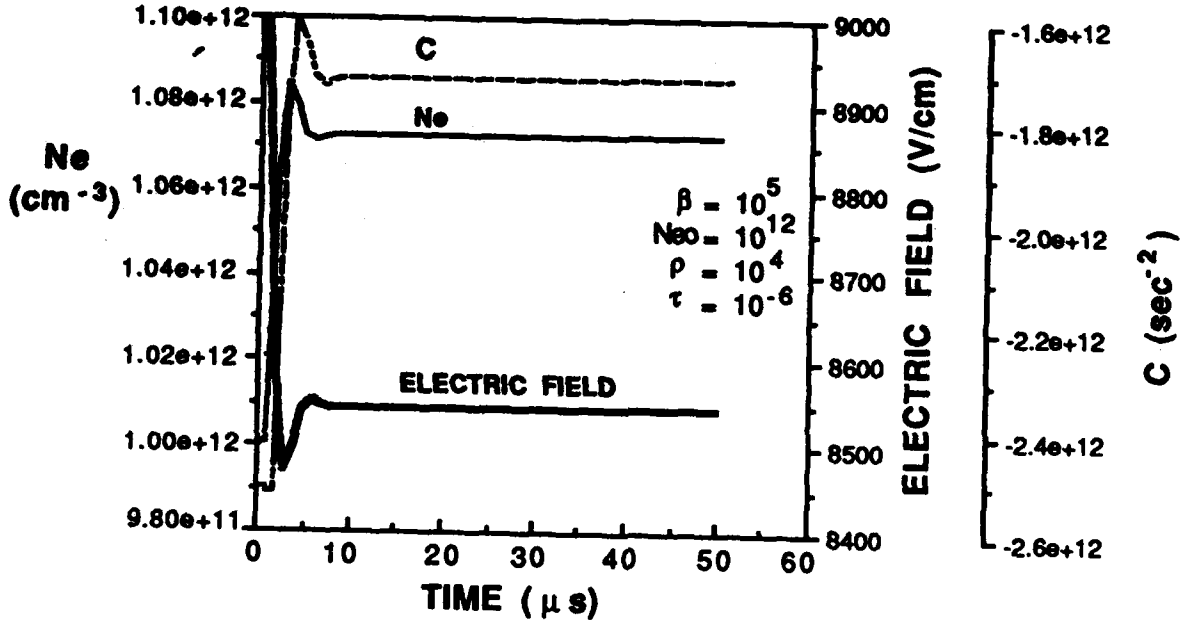

Figure 12 Curves of Ne, E, and C for a volumetrically stable discharge

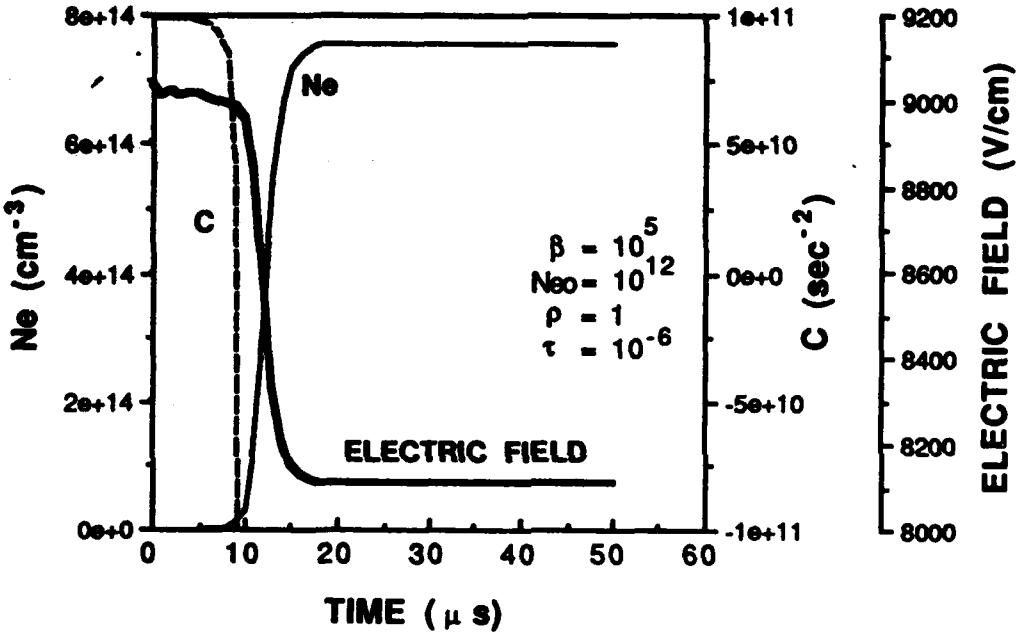

Figure 13 Curves of Ne, C, and E for unstable discharge

density suddenly increases by almost three orders of magnitude after 10 μs. The discharge becomes stable at this large value of $n_e \sim 8 \times 10^{14}$ cm^{-3}. As discussed in the preceding pages $|B|$ increases linearly with n_e and hence the discharge will once again become volumetrically stable at the large value of n_e. Also, C becomes negative at these values of n_e which is consistent with a stable discharge. However, in practice any spatial nonuniformities in n_e could result in streamer formation during this transition.

4.0 INDUCTIVE DISCHARGE STABILIZATION

(Stabilization Against Streamer Formation)

So far the volumetric stability of the discharge has been analyzed. Although a discharge can be volumetrically stable, micro instabilities and nonuniformities can lead constriction of the discharge and streamer formation. To stabilize the discharge against streamer formation SRL proposes to use an RF source. Since a streamer is far more inductive than the discharge, its formation and growth will be inhibited by using RF.

The effectiveness of inductive discharge stabilization can be evaluated from analysis of the equivalent circuit shown in Fig. 14. The discharge impedance, which has inductive and resistive components L_p and R_p while operating stably, is driven by an oscillating current source. The currents through these components are I_L and I_R respectively. The voltage drop across the inductor and resistor must be equal hence

$$i\omega L I_L = R\, I_R \tag{22}$$

By conservation of current,

$$I_L + I_R = I \tag{23}$$

where I is the total current. Equations (22) and (23) can be solved simultaneously to give

STABILIZATION OF DISCHARGE BY INDUCTANCE

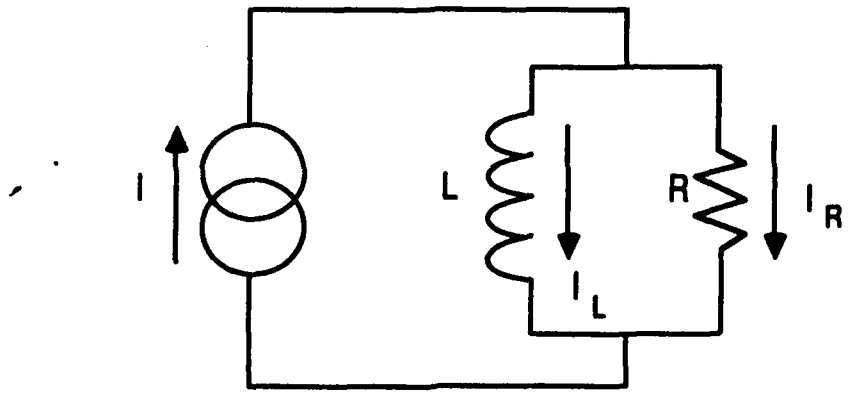

Figure 14

$$I_L = \frac{R(R - i\omega L)}{R^2 + \omega^2 L^2} I \qquad (24)$$

and

$$I_R = \frac{\omega^2 L^2 + i\omega RL}{R^2 + \omega^2 L^2} I \qquad (25)$$

For efficient discharge pumping the inductive current should be minimized, i.e., $R << \omega L$, and $I \simeq I_R$. If the reverse is true then $I \simeq I_L$ and the transfer of energy to the discharge will be very inefficient especially if additional resistive losses are present in the system.

Should the discharge begin to constrict, the inductance will increase and the resistance will decrease. Under these conditions the frequency of RF modulation can be chosen to inhibit arc formation.

From Eq. (22) it is clear that the RF frequency, f, should be selected such that

$$\frac{R_D}{2\pi L_D} > f > \frac{R_s}{2\pi L_s}$$

where R_s and L_s are the resistance and inductance of the perturbed discharge region. These constraints on the modulation frequency have a simple physical explanation. The constraint,

$$\frac{R_D}{2\pi L_D} > f,$$

insures that the skin depth at the modulation frequency is larger than the transverse dimension of the discharge. This constraint leads to spatially uniform pumping of the laser medium. On the other hand, the

constraint

$$\frac{R_s}{2\pi L_s} < f$$

insures that the skin depth at the modulation frequency is smaller than the transverse dimension of the discharge constriction. Therefore, oscillating discharge power is prevented from penetrating to the center of the constricted region. Regions of ionization instability in CO_2 laser discharges are most likely dominated by multistep ionization processes discussed in the preceding section. In this case, the ionization rate, ν_i, is not simply a function of the effective electric field, E/N, but is a function of the power density deposited into the discharge E.J/N. Consequently the limited power flow into the constricted discharge region reduces the ionization rate in that region and enhances stability.

The intrinsic inductance of the discharge can be estimated from the geometrical considerations shown schematically in Fig. 15. Also shown in Fig. 15 is the shape of the magnetic field for the symmetric current condition with no electron density perturbations. The discharge inductance is defined as

$$L_D = \frac{\int B.ds}{I}$$

For a square aspect ratio (i.e., ℓ = h in Fig. 15)

$$L_D = \frac{\mu_0 \ell^2}{4L} \qquad (26)$$

INTRINSIC INDUCTANCE OF DISCHARGE

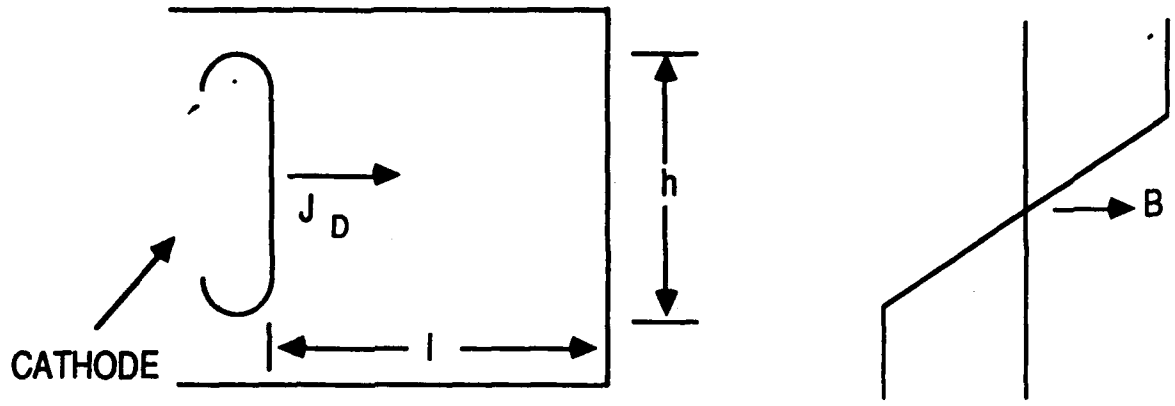

Figure 15

where L is the length of the active volume in the lasing direction and μ_0 is the permeability of free space.

The inductance of the streamer representing the electron density perturbation can be calculated in a similar manner. The geometry of the streamer is shown in Fig. 16. Assuming that the streamer collapses to a radius a

$$L_s \simeq \frac{\mu_0 \ell}{2\pi} \ln \frac{2\ell}{a} \tag{27}$$

Dividing Eq. (27) by Eq. (26) one gets

$$L_s/L_D \sim \frac{2}{\pi} \frac{L}{\ell} \ln \frac{2\ell}{a}$$

Typically ℓ = 0.15 meters, $\ell n\ 2\ell/a \sim 4$ and $L_s/L_D \sim 20$.

To calculate the required frequency of modulation the resistance of the CO_2 discharge must be estimated. The conductivity of the discharge is typically 3×10^{-2} mhos/m. For a discharge cross section of 1.5×10^3 cm^2 and a discharge length, ℓ , of 0.15 meters, the discharge resistance is 35 ohms. The inductance as given by Eq. (26) is 7 nH. So the RF modulation frequency should be in the range

$$5.3 \times 10^7 \frac{R_s}{R_D} \text{ Hz} < f < 8 \times 10^8 \text{ Hz} \tag{28}$$

The upper limit on modulation frequency, 800 MHz, insures that the skin depth of the discharge current is larger than the transverse dimension of the discharge so that the laser medium is pumped uniformly and efficiently. The remaining inequality relates to

INDUCTANCE OF CONSTICTED DISCHARGE

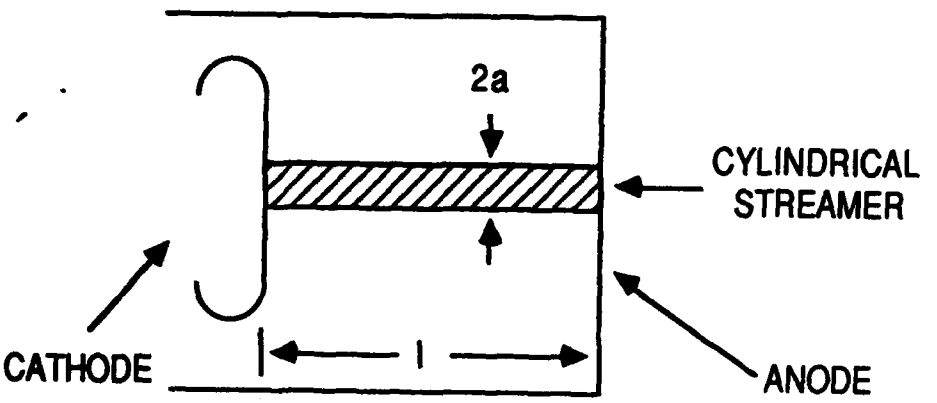

Figure 16

inductive stabilization of constrictions in the discharge current. This inequality insures that the oscillating portion of the discharge current does not contribute to the current in the constricted region. The utility of this inequality is best understood by rewriting it as

$$\frac{R_s}{R_D} < \frac{f}{53} \text{ MHz}$$

This inequality relates the streamer resistance (normalized to the stable discharge resistance) to the modulation frequency required to insure that the oscillating current does not flow through the streamer. Initially, in the stable discharge regime R_s is infinite and therefore $R_s/R_D >> f/53$ MHz. As the discharge constricts, R_s/R_D falls below f/53 MHz and the oscillating current is cut off from the constricted region. At this point, the excess electron density in the constricted region should rapidly recombine thereby driving the discharge back to stable operation. If the modulation frequency in this example were chosen to be 50 MHz, then stabilization should begin to occur when the streamer resistance begins to drop below the discharge resistance, i.e. as the streamer begins to form.

5.0 EFFECT OF RF MODULATION ON CO_2 LASER OPERATION

The RF modulation will have an impact on discharge and laser parameters such as electron density, temperature and small signal gain. These effects will be briefly discussed below.

The electron production and loss rate is given by

$$\frac{dn_e}{dt} = S + \nu_i n_e - \alpha n_e^2 - \beta n_e \qquad (29)$$

For a self sustained discharge, S=0. Typically, CO_2 laser discharges are recombination dominated. Because of the RF modulation, the discharge electric field will vary in time. The electron temperature and recombination rate will also vary. As the electric field decreases the average electron energy decreases and recombination rate increases which will have a stabilizing effect and allow slightly constricted regions in the discharge to recover to the ambient electron density.

It is desirable to keep the electron density constant in time. From Eq. (29) it is clear that, for $\beta << \alpha n_e$, the electron density will be constant if $f >> \alpha n_e$. Typically, $n_e \sim 10^{12}$ cm^{-3} and $\alpha \sim 10^{-6}$ cm^3/sec (see Fig. 7). So if $f >> 1$ MHz, which is consistent with the modulation frequency given by (28), n_e will be essentially constant.

The RF electric field will cause variations in the average electron energy. Such variations result in inefficiencies because of nonoptimal pumping of N_2 vibrational levels (see Fig. 5). The electron temperature will be nearly constant if the RF frequency is

$$f >> k_e N_a$$

where k_e is the electron impact excitation rate of ground state N_2 and N_a is the N_2 density. Typically $k_e \simeq 5 \times 10^{-9}$ cm^3/sec and $N_a \simeq 5 \times 10^{18}$ cm^{-3} and therefore $f > 2 \times 10^{10}$ Hz. Since the RF modulation frequency will certainly be lower than 10^{10} Hz the average electron energy will follow the modulation frequency in time.

For the small signal gain to be constant, $f >> k_e N_c$, where

k_e ($\sim 10^{-12}$ cm^3/sec)[1] is the vibrational transfer rate from N_2 to CO_2 and $N_c \simeq 10^{19}$ cm^{-3} is the CO_2 number density. So for a constant small signal gain $f > 10^7$ Hz. From Eq. (28) the RF modulation frequency will be chosen such that the small signal gain will be constant which is important for maintaining high laser extraction efficiency.

For efficient coupling of power into the laser discharge it is important that the impedence of the discharge does not vary strongly with the RF modulation. The power reflection R from a load having an impedence Z_L is given by

$$R = \left(\frac{1 - Z_0/Z_2}{1 + Z_0/Z_2} \right)^2$$

where Z_0 is impedence of the RF power supply and $Z_L \propto E/en_e v_D$. From the curves shown in Fig. 5 the $v_D \propto (E)^{1/2}$. From Eq. (29) $n_e \propto \nu_i/\alpha$. From Fig. 6 one can see that ν_i is a very strong function of the electric field while α decreases with increasing electric field. So n_e could vary very strongly with the electric field, i.e., $n_e \sim E^7$. Such a strong variation could result in power reflection from the discharge and the overall efficiency of the discharge could be adversely effected. It is in part for this reason that the RF frequency be chosen such that the electron density is constant, i.e. $f \gg \alpha n_e$.

Finally the cross section area of the discharge will be constrained by the skin effect. For a given RF frequency the cross sectional area A must be smaller than a certain value if the current through the cross section is to be uniform. This unequality is given

by

$$A \leq \frac{1}{\pi f \mu \sigma} \tag{30}$$

where σ the conductivity of CO_2 laser discharges is typically $2\text{-}3 \times 10^{-2}$ MHos/M.

From the preceding discussions a scaling map for CO_2 can be drawn such a scaling map is shown in Fig. 17. This figure is a plot of RF frequency vs cross sectional area of the discharge. As discussed earlier the RF frequency should be larger than 30 MHz for the small signal gain and electron density to be constant. On the high end the frequency is constrained by the skin effect. Also shown in Fig. 17 is the expected 10.6 μ laser energy that can be extracted per pulse. From this figure it is clear that this pumping technique can provide enough laser energy for most tactical applications.

CO_2 SCALING MAP

FREQUENCY VERSUS CROSS SECTIONAL AREA

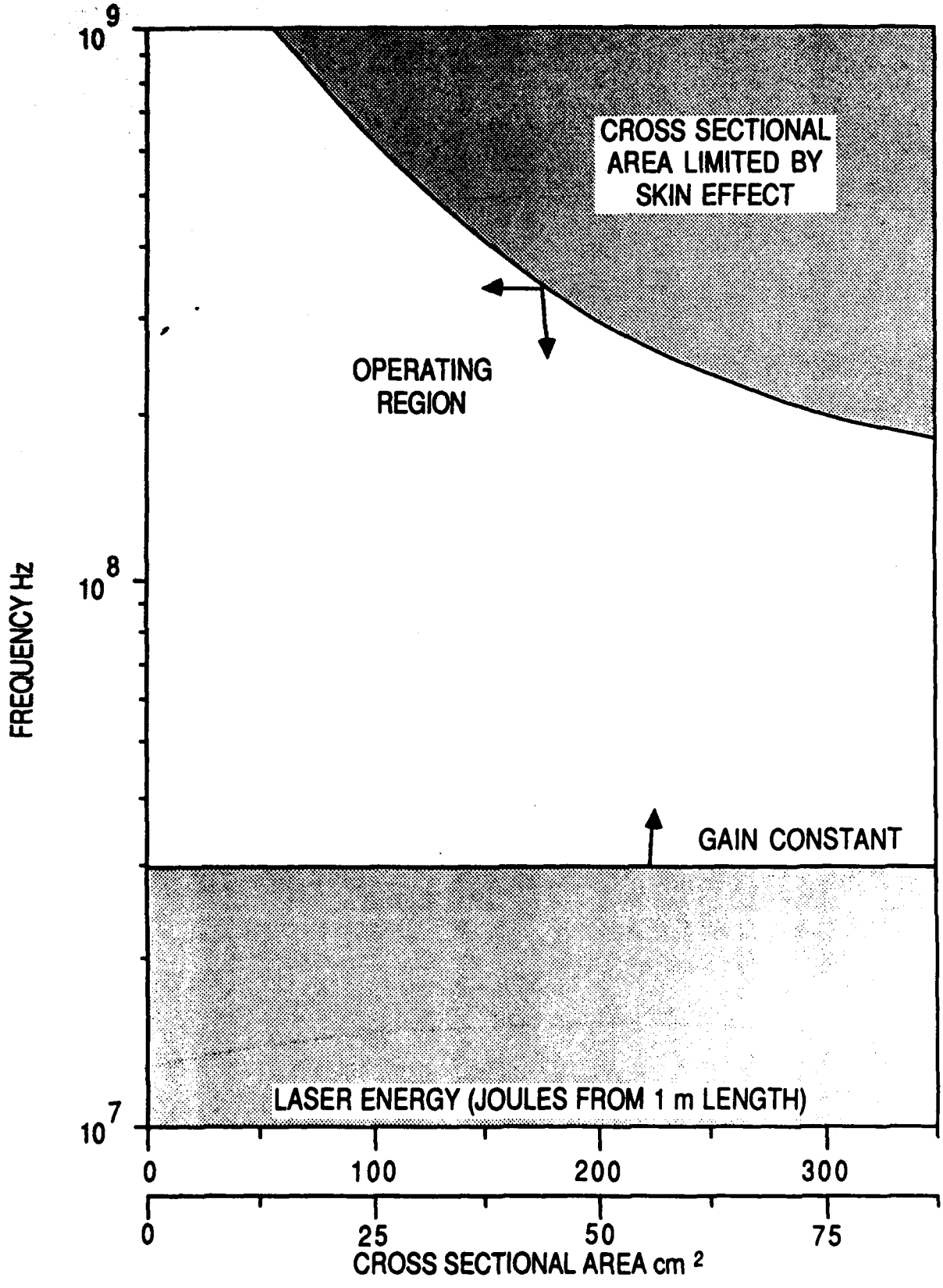

Figure 17

6.0 CONCEPTUAL DESIGN OF SINGLE PULSE EXPERIMENT

The conceptual design of the experiment is sufficiently flexible to allow for variation of the discharge and laser parameters over a broad range to enable determination of the optimum discharge/laser conditions. Specifically the constant current RF power supply can have the following features:

- Variable frequency (10-100 MHz)
- Variable shunt impedence to allow for discharge current variation
- Discharge initiation with a 10 nsec overvoltage pulse having variable delay to the onset of the discharge sustainer pulse. In addition a UV preionizing source will provide an initial uniform density of electrons such a source is discussed later in this section. These features will permit rapid determination of the optimum laser performance within the constraints of ensuring discharge stability.

Figure 18 shows a schematic of the laser discharge and UV preionizer. The discharge cell will be fabricated out of a quartz tube having a diameter of 1 cm (cross sectional area of 0.8 cm^2) and a length of 50 cm. The RF power will be coupled in via a set of external electrodes that will be spaced about 1 cm apart. The RF source will be capable of delivering 6 kV and 20 A and the discharge current will be 0.5 - 1 A/cm^2 and the electric field 5-6 kV/cm. The laser discharge characteristics are given in Table II. From this table one can see that the RF power supply must be capable of delivering 120 kW in a 50 μs pulse.

Also given in Table II are the expected CO_2 laser characteristics

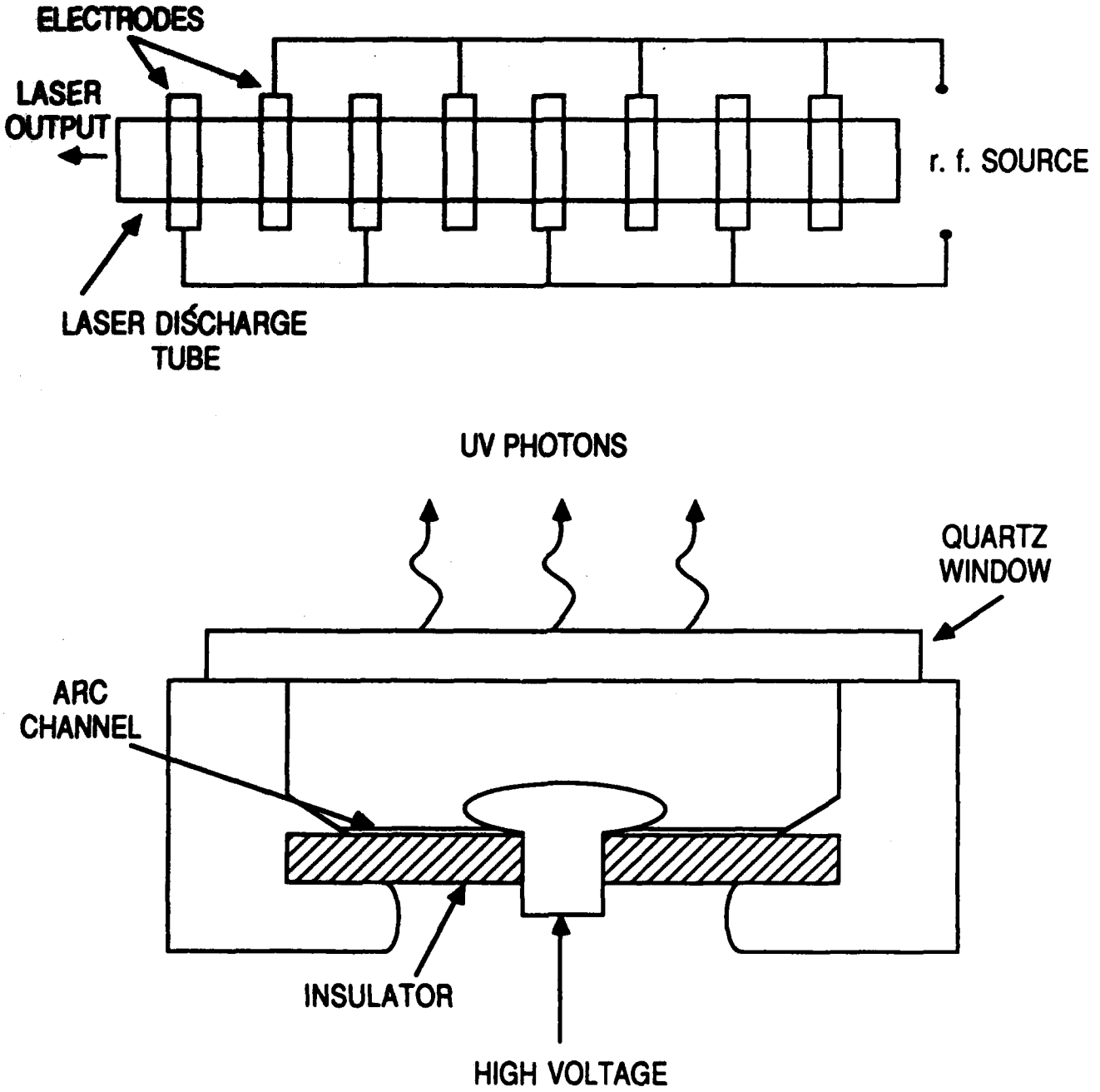

Figure 18 Schematic of laser/discharge tube and surface-spark discharge UV generator

TABLE II

LASER/DISCHARGE CHARACTERISTICS

• DISCHARGE CHARACTERISTICS	
GAS MIXTURE	3/2/1 $He/N_2/CO_2$ AT 1 ATM
TOTAL DISCHARGE CURRENT	20 A/cm^2
CURRENT DENSITY	1 A/cm^2
ELECTRIC FIELD	5-6 kV/cm
PULSE LENGTH	50 μs
INPUT POWER	120 kW
ELECTRON DENSITY	1-2 x 10^{12} cm^{-3}
MEAN ELECTRON ENERGY	1 eV
• LASER CHARACTERISTICS	
GAIN AT 10.6 μm	1-2 x 10^{-3} cm^{-1}
SATURATION FLUX	25 kW/cm^2
LASER POWER EXTRACTION	20 kW
LASER ENERGY EXTRACTED	1 JOULE
• DISCHARGE/LASER CELL	
CROSS SECTIONAL AREA	0.8 cm^2
LENGTH	50 cm
OUTPUT COUPLING	10-20%

for 3/2/1, $He/N_2/CO_2$ gas mixture at a total pressure of 1 atm. The saturation flux for this mixture is 25 kW/cm^2.[2] For the pump power of 120 kW the expected gain is 1-2% per cm.[2] Using a hole coupled copper mirror with a 10-20% output coupling the energy extracted will be about a joule.

To insure a uniform discharge SRL has designed a UV preionization source. Such a preionization is the most convenient because of factors including:

(1) ease of coupling the UV into the discharge

(2) typically UV sources are generated by relatively low voltages (5-10 kV) and hence they can be made compact and light weight

The disadvantage of using UV sources is the uniformity of the preionization is not as good as that generated by x-ray preionization. However, this is not expected to be a significant issue in the present discharge configuration because of the small cross sectional areas.

There are a number of alternative methods for obtaining the UV radiation ultimate choice will depend on the particular application. For long lived space applications, UV generated by rare gas flash lamps may be the most appropriate.[3] These sources are highly efficient for converting electrical power into optical radiation and at 10,000-15,000 ^0K they are efficient radiators in the near UV spectral region.[4]

Another attractive alternative is a vacuum surface spark discharge. The advantage of these UV sources are their simplicity and their efficient radiation in the UV.[4] Figure 18 shows a

schematic of such a source. The radiation is created by a spark along an insulating material such as Al_2O_3 or ZnO_2 and the photons are coupled out of the vacuum chamber through a quartz window. Typically the pulse lengths of the radiation is 5-10 μs.

A block diagram of the constant current power supply is shown in Fig. 19. The constant current supply is provided by a push-pull cathode follower circuit using two 4PR1000 tetrodes. From the characteristics of these tetrodes shown in Fig. 20, it can be seen that the current is constant for plate voltage between 3-14 kV. The RF power will be coupled to the discharge via a transformer and the output will provide constant current pulses of up to 20 amperes for voltages up to 6 kV.

The power supply design is conservative and the tubes were chosen to be rugged enough to absorb all the RF power should fault modes develop as the limits of discharge stability are explored. Further, the circuit is capable of generating an initial overvoltage prepulse to initiate the discharge.

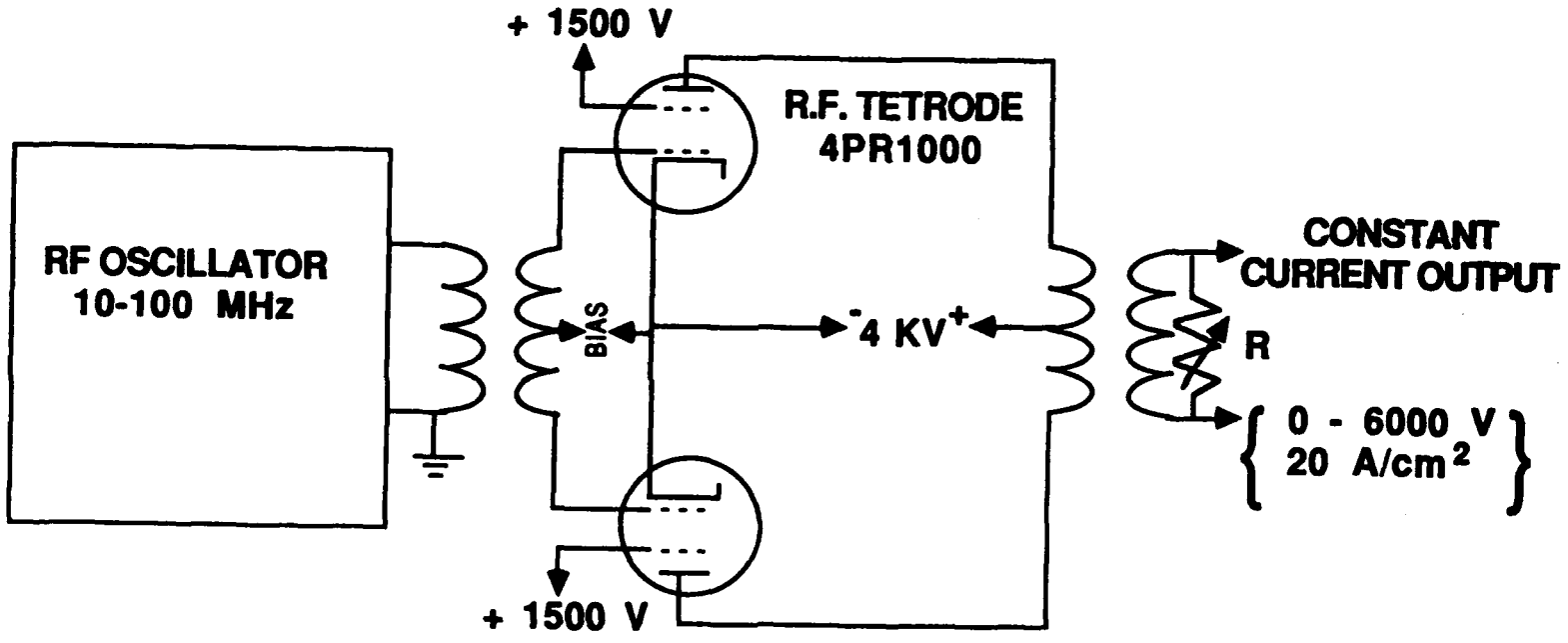

Figure 19 Constant current 10-100 MHz power supply

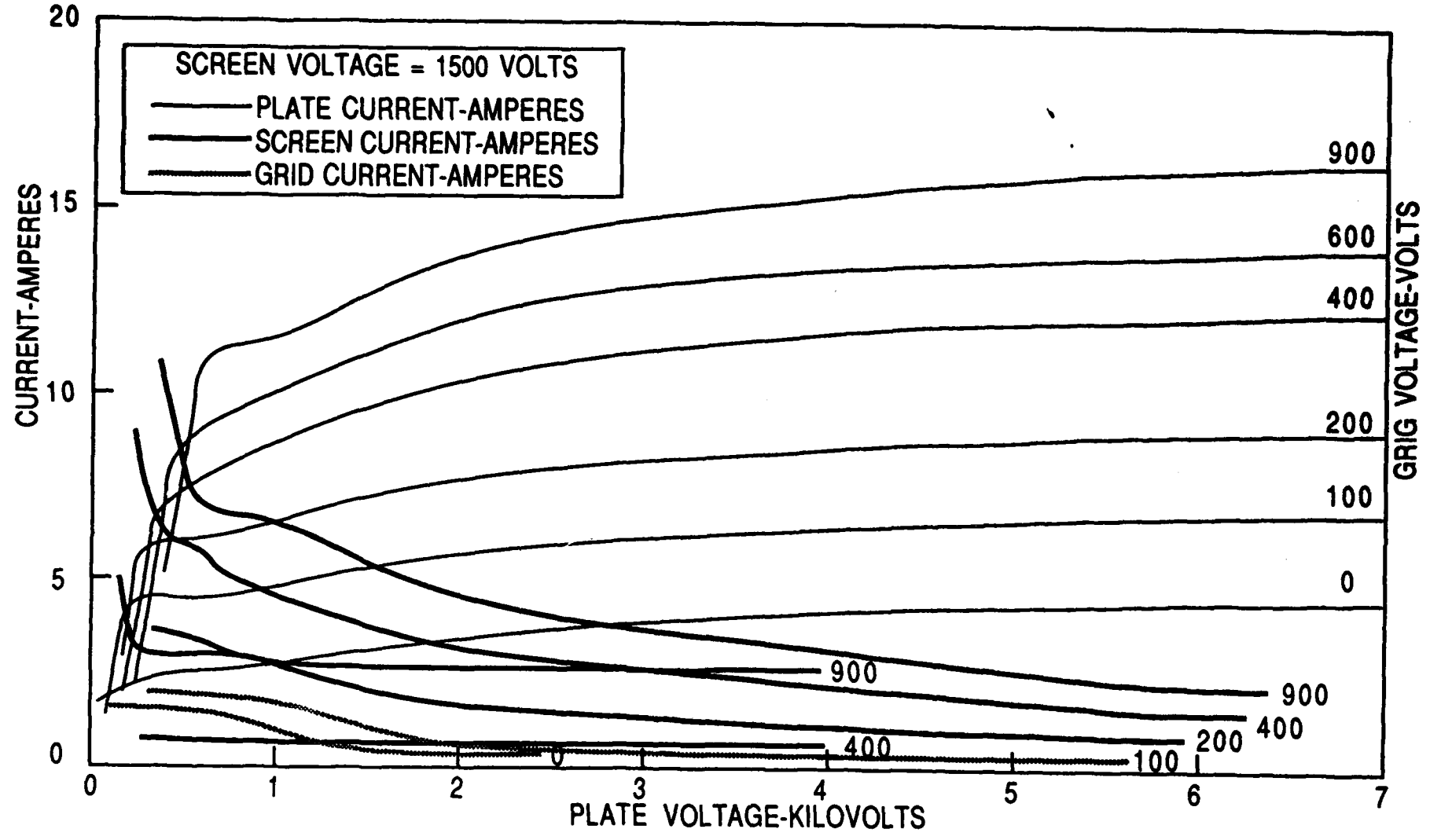

Figure 20 Typical tetrode plate characteristics

7.0 SUMMARY

The stability of CO_2 laser discharges have been analyzed analytically and numerically. The discharge model includes the electrical circuit. It is clear from the analysis that a current source is more stable than a voltage source. Further by the use of RF discharge streamer formation can be inhibited. Scaling maps have been presented that identify regions of stable discharge operation.

In the last section of this report a conceptual design of an experiment to verify the stability model is presented. The experimental design is flexible enough to permit both discharge and laser experiments.

REFERENCES

1. G.E. Caledonia, et al., "Analysis of Metastable State Production and Energy Transfer," Report #AFWAL-TR-86-2078 (1986).
2. D.H. Douglas-Hamilton and R.S. Lowder, AERL Kinetics Handbook, (1974).
3. B. Smith and F. Schula, "Flashlamps for Pulsed Solid State Lasers," Engineering Note #156, ILC Technology, Inc., Sunnyvale, CA (August 16, 1982).
4. K.D. Ware, T.M. Johnson and C.R. Jones, "Surface-Spark Discharges Compared with Exploding Wires/Films as High Temperature UV Source," Fourth IEEE Pulsed Power Conference, p. 507 (1983).